Revista Argentina de Clínica Psicológica
2020, Vol. XXIX, N°4, 933-940
DOI: 10.24205/03276716.2020.1504

Application and Clinical Value of 3.0T Magnetic Resonance Whole Heart Coronary Angiography in the Diagnosis of Coronary Artery Stenosis

Songhong Yue[a#*], Junting Tang [b,#], Gaimei Wang[b], Jing Zhang[a], Wanjun Hu[a], Juan Liang[a], Yuping Bai[a]

Abstract

Object: To study the clinical value of 3.0T magnetic resonance whole heart coronary angiography in the diagnosis of coronary artery stenosis.

Method: 38 patients with suspected coronary artery stenosis were randomly selected from our hospital from September 2017 to September 2018. All patients were diagnosed with whole heart coronary angiography by 3.0T magnetic resonance examination. Angiography was adopted as the gold standard to evaluate the value of whole heart coronary angiography via 3.0T magnetic resonance. All the 38 patients have completed the examinations, including 13 segments with grade 0 image quality and 28 segments with grade I image quality. Of 38 patients, 25 underwent coronary angiography, 29 of 25 patients had coronary artery stenosis, while 30 of 25 patients had coronary artery stenosis.The results of 22 coronary stenoses which were confirmed by coronary angiography are consistent with the results obtained from whole heart coronary stenosis by 3.0T MRI. The accuracy, sensitivity, specificity, negative predictive value and positive predictive value of the imaging scheme were 75.86%, 75.86%, 96.67%, 73.33% and 80.00%, respectively.The 3.0T MR whole heart coronary angiography is of outstanding value in the diagnosis of coronary artery stenosis and is worthy of utilization.

Keywords: Coronary artery stenosis; Diagnosis; 3.0T magnetic resonance whole heart coronary angiography; Application; Clinical value

1. Introduction

Coronary artery stenosis is a common disease in cardiovascular system, which directly endangers the life of patients that cause by many environmental and external factors Feng et al., 2020; Liu et al., 2018; Su et al., 2020; Su et al., 2019; Duan et al., 2020; Zhong et al., 2020; Zuo et al., 2015; Zuo et al., 2017; Chen and Xu, 2020; Liu et al., 2017; Jiang et al., 2020; Pan et al., 2020; Chen et al., 2020; Zuo et al., 2013; Li et al., 2020; Liu et al.,2020; Wang et al.,2019; Xu et al., 2019; Zhang et al., 2019; Zhang et al., 2019). Most heart disease risk factors are influenced by lifestyle and environmental factors. In recent decades, heart attacks in both women and men have declined due to improved eating habits and smoking cessation. This rate has remained constant in recent years due to the increasing incidence of obesity in the United States and industrialized countries (Liu et al., 2019; Gou et al., 2019; Xu et al., 2019; Zhu et al., 2019; Zhao et al., 2019; Xiao et al., 2019; Kamran et al., 2019; Li et al., 2019; Xu et al., 2019; Wan et al., 2019; Mou et al., 2019; Si et al., 2019; Zhou et al., 2019; Irshad et al., 2019; Bhatti et al., 2019; Yan et al., 2019; Loya-Rivera et al., 2019; Huang et al., 2019; Gao et al., 2019; Zhou et al., 2019).

Timely diagnosis and treatment are important measures to improve the condition and prognosis of patients with coronary artery stenosis (Ma et al., 2017). In recent years, with the continuous improvement of diagnostic technology at home and abroad, a new non-invasive MR coronary angiography scheme has been introduced in clinical diagnosis, At present, the 3.0T MR whole heart coronary angiography scheme has been involved in the diagnosis of coronary artery stenosis patients in our hospital. In order to analyze its effect, 38 patients with suspected coronary artery stenosis

[a]Department of Magnetic Resonance, Lanzhou University Second Hospital, Lanzhou730000, Gansu , China
[b]Department of Magnetic Resonance,Linfen People's Hospital, Shanxi 041000, China
**Corresponding author: Songhong Yue*
E-mail: 793343312@qq.com
[#]These authors have contributed equally to this work.

were randomly selected from our hospital from September 2017 to September 2018.

2. Materials and Methods

2.1. Clinical Data

Thirty-eight suspected patients with coronary artery stenosis admitted to our hospital from September 2017 to September 2018 were randomly selected. There were:20 (52.63%) males and 18 (47.37%) females; age were ranged from 40 to76 years old with a median of 58.82±2.87 years old; ECG were performed for all the patients which reported which sinus rhythm and the heart-rate was ranged from 68/min-80/min, of which 25 patients developed coronary symptoms within two weeks after admission. The arteriography inclusion criteria were patients or family members had known the research activities and signed informed consent; exclusion criteria were any contraindications of 3.0T magnetic resonance whole heart coronary angiography.

2.2. Examination Protocol

Thirty-eight patients with coronary artery stenosis had received magnetic resonance whole heart coronary angiography with a 3.0T magnetic resonance image machine ((Philip, Ingenia 3.0T, USA). The gradient field intensity was set at 30 mT/m, and the gradient switching rate was 150 mT/m per second with 16 channel phased array coils. During the examination, a 3D-TFE sequence is selected and then combined with real-time breath gating navigation. Vector ECG vector R-wave triggers the gating technique. During the examination, the patients were assisted in maintaining a supine state and scanned by the transverse axis. Four-chamber heart film data were obtained, the image information was observed, the motion amplitude of right coronary artery tissue in middle and late diastolic phase was subsequently determined, and the time interval of which the motion amplitude was the smallest has been determined. The acquisition window width was set to determine the trigger delay time (TD t) in the examination. The K-space fast gradient echo factor, i.e. the ratio of acquisition window width to TR, ~~is~~ was calculated. Then the patients were scanned with MR coronary imaging sequence, and the scanning range was set to the bifurcation of pulmonary artery to the base of the heart. The scanning mode was set to 3D mode, FOV was 300 x 250 mm, the scanning layers were 120-140 layers, the acquisition voxels were set to 1.25 x 1.25 x 1.6, the reconstructed voxels were set to 0.62 x 0.8, and the inversion angle was15 degrees. The echo time was 70 ms, and the frequency-selective fat suppression could enhance the contrast of coronary artery signals. The 3.0T magnetic resonance whole-heart coronary angiography was interpreted by imaging physicians to quantitatively analyze and grade the stenosis degree of each segment of coronary artery lumen in patients with specific software. The stenosis can be judged as significant if the angusty degree was greater than 50%, it (Lee et al., 2017).

2.3. Analysis of the images

After transferring the 3.0T MR whole heart coronary angiography image to the post-processing workstation of the diagnostic department, the post-processing was performed via a software of *Soap-Bubble tool* (Philips, USA) with the multiplanar reconstruction technology. The coronary artery tissue was divided into nine segments, and the image quality was evaluated objectively. The nine segments were proximal left circumflex coronary artery, distal left circumflex coronary artery, main left coronary artery, proximal right coronary artery, middle right coronary artery, distal right coronary artery, proximal left anterior descending coronary artery, middle left anterior descending coronary artery and distal left anterior descending coronary artery (Luo et al., 2018). During the evaluation of the image qualities of the 3.0T MR whole-heart coronary angiography, the four-point system was adopted: vascular tissue could not be displayed was scored 0; vascular tissue could be displayed, but could not be accurately diagnosed, scored 1; vascular tissue edge was blurred, but could be diagnosed, scored 2; vascular tissue had high clarity, and only a few artifacts appeared, were scored with 3 and 4 points, respectively (Li et al., 2017; Zhang et al., 2018), and no artifacts in the vascular tissue. The image quality evaluation work was assessed by two professional specialties. When the score is consistent, the final score can be regarded as a result. If the image quality evaluation result was greater more than 2 points, it could be identified that the image has the diagnostic value. Coronary artery tissue was evaluated by double-blind method, and the presence of stenosis was observed. If one or more coronary artery had stenosis, it would be positive (Shao et al., 2018).

2.4. Statistical Analysis

The data statistics in this study were all performed by SPSS20.0 software, [n (%) was the counting data, and χ^2 test was adopted; (+s) was the measurement data, and t-test was utilized. The results showed that there was a significant

difference (P < 0.05).

3. Result

All the 38 patients completed the examination, including 13 segments with grade 0 quality and 28 segments with grade I quality, as shown in Table 1(Tables 1 -2).

Table 1. **Examination results of patients with coronary artery stenosis**

		LADimage			RCAimage			LCXimage	
		Near segment	Middle part	Far segment	Near segment	Middle part	Far segment	Near segment	Far segment
Imaging score	3.69±0.47	3.66±0.47	3.18±0.67	2.49±0.77	3.69±0.47	3.38±0.56	2.79±0.86	2.19±0.88	1.18±0.73

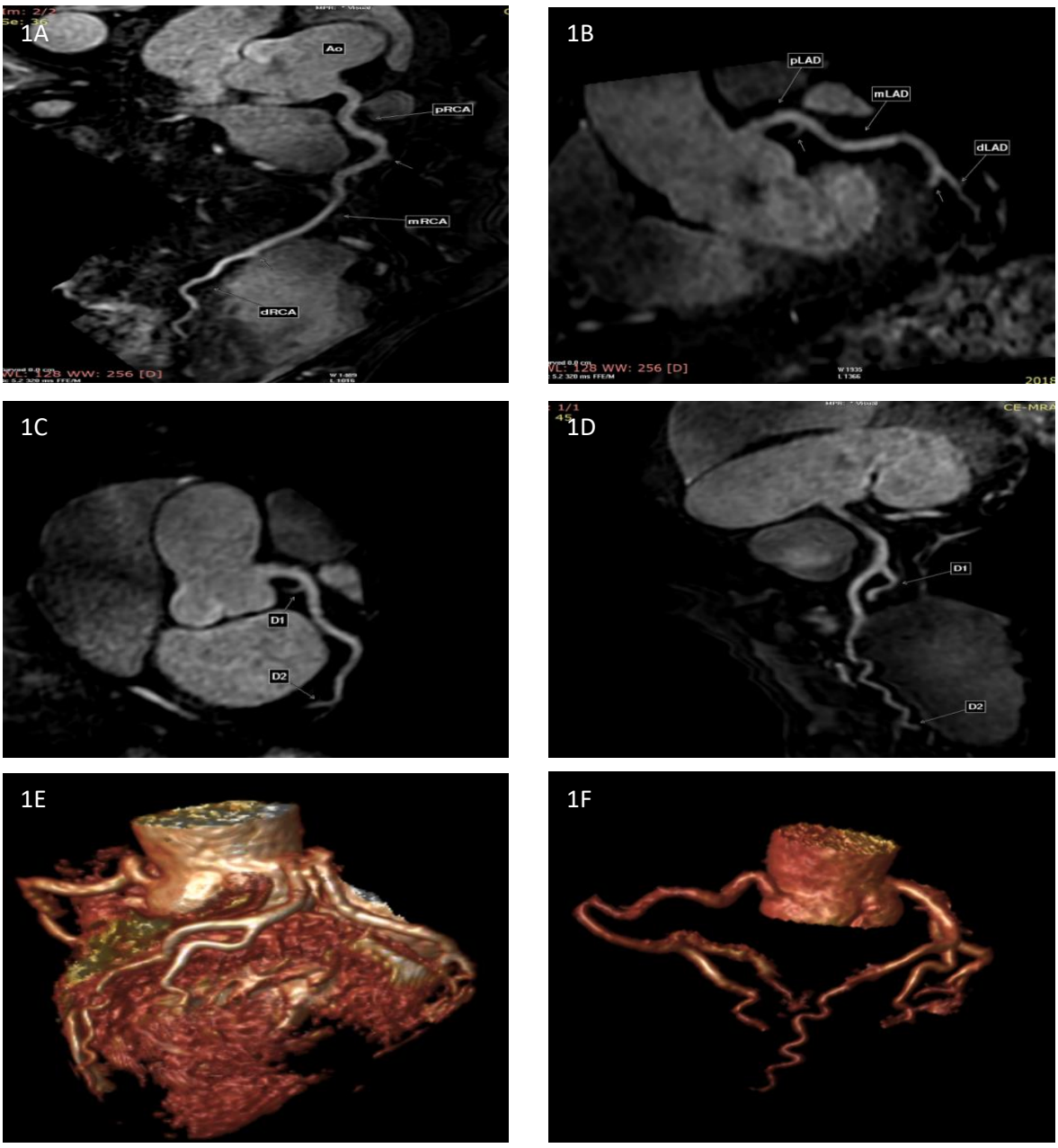

Figure 1. **A MPR image of CMRA right coronary artery showed the full length of the right coronary artery, the distal, middle and proximal segments are clear, and the edge of the wall is smooth and sharp； 1B. CMRA-MPR showed distal and proximal segments of left coronary artery； 1C-1D. CMRA-MPR showed the first and second diagonal branches of LAD in different directions;1E-1F. CMRA-VR showed main branches of the left and right coronary.**

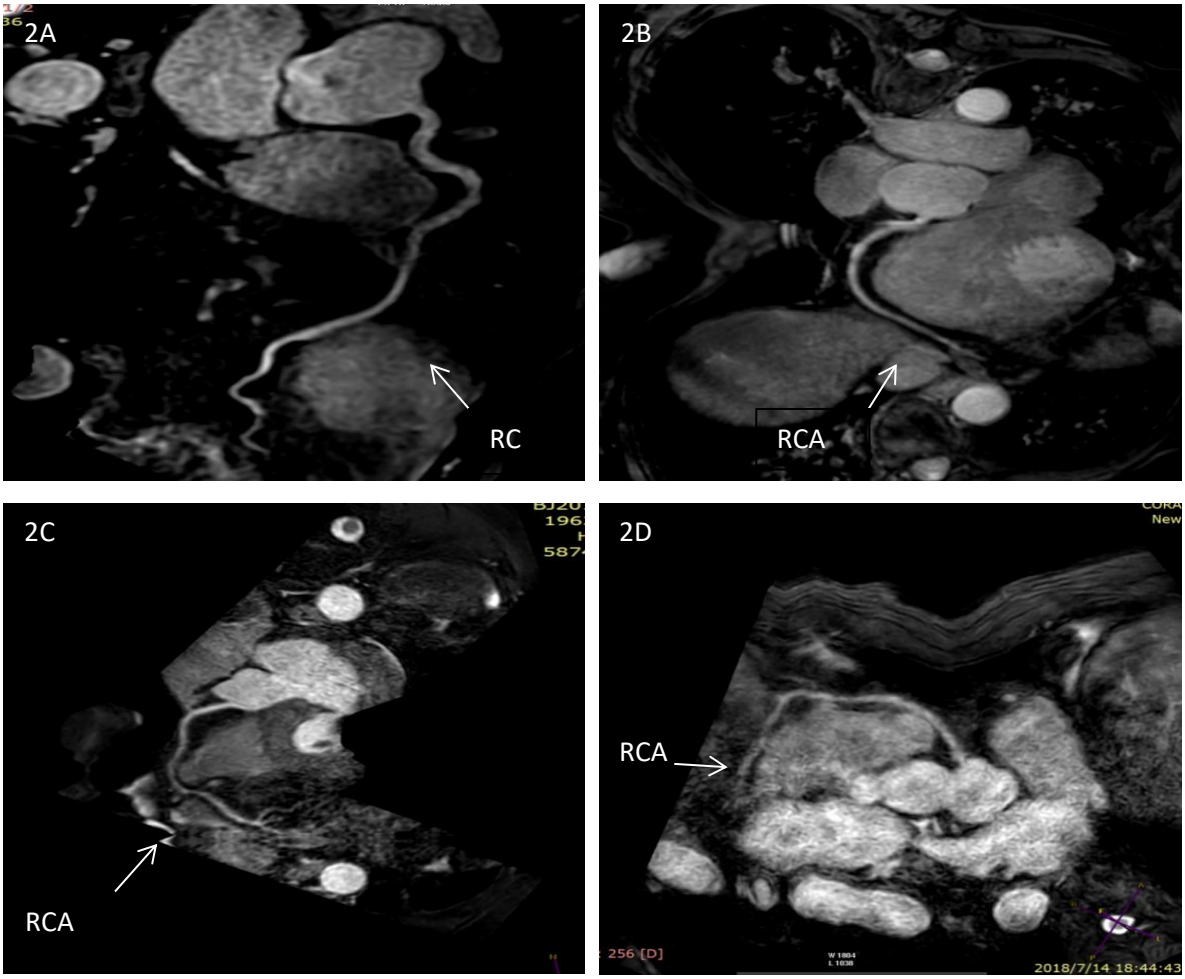

Figure 2. **Schematic diagram of image quality scoring; Take RCA as an example; A.4 score： The blood vessels are clearly developed, and the edges are sharp and smooth； B.3score： The blood vessels are clearly formed, and the edges are slightly blurred； C.2 score Visible blood vessels running, moderately blurred edges； D.1 score： Severe artifacts, the blood vessel wall is blurred or cannot be displayed, and cannot be assessed.Of the 38 patients, 25 underwent coronary angiography, and 29 of the 25 patients had stenosis. Among them, 12 patients had single-vessel disease, 7 patients had double vessel disease and 1 patient had the three-vessel disease. Thirty coronary artery stenosis was found in 25 patients following magnetic resonance whole-heart coronary angiography in 38 patients. The detection results of 22 coronary artery stenosis were consistent with those of coronary angiography. The accuracy, sensitivity, specificity, negative predictive value and positive rate of 3.0T magnetic resonance whole-heart coronary angiography were 75.86%, 75.86%, 96.67%, 73.33%, respectively. The predicted value is 80.00%, as shown in** Table 2.

Table 2. **Diagnostic efficacy of coronary angiography**

Accuracy	Sensitivity	Specificity	Negative predictive value	Positive predictive value
75.86%	75.86%	96.67%	73.33%	80.00%

4. Discussion

3.0T magnetic resonance whole-heart coronary artery imaging (3.0T MRCAI) was developed in the 1980s. It is a non-invasive measure to examine the health status of coronary artery tissue. With the further innovation of imaging methods and imaging sequence in recent years, 3.0T MRCAI has been applied in various medical institutions (Multinational et al., 2018; Albrecht et al., 2017). Not only can the 3.0T magnetic resonance whole-heart coronary angiography demonstrate non-traumatic characteristics, it also features with radiation-free, which can achieve imaging objectives at any level. By combining with delayed enhanced imaging and cine imaging, it can reveal both of the patients' cardiac structure their as well

as cardiac function, myocardial viability and myocardial perfusion.At the same time, we can estimate the stable state of atherosclerosis and the specific condition of abnormal coronary artery tissues in aortic-coronary artery bridging vessels(Ran et al., 2017; Zhou et al., 2017).

The application of 3.0T magnetic resonance whole-heart coronary angiography in the diagnosis of coronary artery stenosis enables patients to undergo an examination under free-breathing conditions and scan their whole hearts under high-resolution three-dimensional volume conditions. The recovery of T2 pre-pulse sequence and pulse sequence inversion is utilized to make the blood and adjacent tissues of patients contrast. The effects of physiological movement in patients were suppressed by the combined application of ECG vector gating, three-dimensional motion-following measures and respiratory navigation echo techniques in order to improve the performance of this technique. The signal acquisition link is expanded by 3D steady-state fast echo sequence, which can improve the quality of new coronary artery imaging and achieve high contrast imaging targets such as fast imaging and high signal-to-noise ratio imaging (Wang et al., 2018; Zhang et al., 2017; Li et al., 2017; Lu et al., 2017). After examining 38 suspected patients with coronary artery stenosis with 3.0T magnetic resonance whole-heart coronary angiography, 13 segments with grade 0 imaging quality were found, 28 segments with grade I imaging quality was found, and 29 coronary artery tissues in 20 patients with coronary artery stenosis were found in 25 patients who underwent coronary angiography. The results of 3.0T MR whole heart coronary angiography showed that the accuracy, sensitivity, specificity, negative predictive value, negative predictive value and positive predictive value of 3.0T MR whole heart coronary angiography were 75.86%, 75.86%, 96.67%, 73.33%, 80.00%, respectively. The application value of coronary angiography can be used in the clinical diagnosis of coronary artery stenosis.

5. Conclusion

The current MR angiography protocol incorporates several improvements over those used in earlier studies. In details, the contemporaneity coronary MR angiogram has been derived in a double-slanted three-dimensional plane, following a process of major coronary arteries that requires repeated MR acquisition to cover the entire coronary artery: 1. A steady state, free-floating MR sequence allows the acquisition of a large three-dimensional volume covering the entire heart without affecting the artery's higher luminal signal. 2. Planning of the three-dimensional volume of whole-hearted coronary MR angiography is very simplified and considerable time gains can be obtained by eliminating the 3-point planning required for biaxial three-dimensional coronary MR angiography. 3. Prospective ECG clinic has been used to correct cardiac motion on coronary MR angiogram by obtaining imaging data in the mid-diastolic period. Favorable coronary images were obtained in patients with a heart rate of 70 beats/min by reconstructing the images at mid-diastole. However, in patients with higher heart rates, reconstruction at an earlier stage of the cardiac cycle is essential. In the current study, the minimum motion interval of the RCA was visually determined on a cine MR image, thereby utilizing coronary MR data in all patients. The use of patient-specific acquisition windows during the cardiac cycle reduces motion blur on coronary MR angiograms, providing the examiner with diagnostic coronary MR images even in patients with relatively high heart rates.

There are some limitations existing in the research: current evaluation has been completed by 2 experienced radiography specialists, which means the real evaluation effect may depend on the interpretation level in certain degree. 2. Failure of MR acquisition is likely to occur in the daily scan operations, the design and data analysis did not make such situation involved, where may lead to the result inaccuracy; 3. Compare to invasive angiography as well as coronary CTA, the spatial resolution of MR angiography is relatively lower, and the imaging time is still long, which reflexes the need of experienced interpreters as well as radiography specialists to make correct diagnosis. Nevertheless, the reported sensitivity and negative predictive value of the current whole-heart coronary MR angiographic approach may not as favorable as of that from 256-slice computerize tomography, which demonstrates significant greater special resolution. In the meantime, it is likely eliminate certain emergency cases since the long examination time. Third, the heart commonly moves by the diaphragm in vertical direction.

Alone with previous and current investigations, all the features and improvement of the techniques have significant facilitated the clinical application for the diagnosis of coronary artery stenosis. That is, in this study, whole-heart coronary MR angiography has been validated for the diagnosis with noninvasive detection of significant luminal narrowing in the coronary artery. Although multicenter studies are desirable to further support

the diagnostic value of coronary MR angiography, it has already demonstrated with considerable sensitivity and high specificity, which deserves to be widely utilized in the clinical setting.

Acknowledgements

This work was supported by Lanzhou Scienceand Technology PlanProject (2017-4-61).

References

[1] Albrecht, M. H., Varga-Szemes, A., & Schoepf, U. J. (2017). Coronary artery assessment using self-navigated free-breathing radial whole-heart magnetic resonance angiography in patients with congenital heart disease. *European Radiology, 28(03)*:1-9.

[2] Bhatti, H., Jawed, R., Liu, H., Ali, I., Zhu, L., & Liu, Q. (2019). Clear discrimination of single-molecule of a single-stranded DNA homopolymers and hetero-homopolymers through a new mutant of mycobacterium smegmatis Porin A, MspA. Nanoscience and Nanotechnology Letters, 11(8), 1104-1115.

[3] Chen, H., Chen, A., Xu, L., Xie, H., Qiao, H., Lin, Q., & Cai, K. (2020). A deep learning CNN architecture applied in smart near-infrared analysis of water pollution for agricultural irrigation resources. Agricultural Water Management, 240, 106303.

[4] Chen, L., & Xu, X. (2020). Effect evaluation of the long-term care insurance (LTCI) system on the health Care of the Elderly: a review. *Journal of Multidisciplinary Healthcare*, *13*, 863.

[5] Duan, F., Hu, M., Guo, C., Song, Y., Wang, M., He, L., Zhang, Z., Pettinari, R., & Zhou, L. (2020). Chromium-based metal-organic framework embedded with cobalt phthalocyanine for the sensitively impedimetric cytosensing of colorectal cancer (CT26) cells and cell imaging. Chemical Engineering Journal, 125452.

[6] Feng, Q., Li, Y., Wang, N., Hao, Y., Chang, J., Wang, Z., Zhang, X., Zhang, Z.,& Wang, L. (2020). A Biomimetic Nanogenerator of Reactive Nitrogen Species Based on Battlefield Transfer Strategy for Enhanced Immunotherapy. Small, 2002138.

[7] Gao, G., Yao, Z., Chen, Z., Shi, X., Shen, J., Shen, L., & Yu, J. (2019). Prognostic Role of EphA4 in Various Human Cancers: A Meta-Analysis of 11 Related Studies. Nanoscience and Nanotechnology Letters, 11(8), 1160-1165.

[8] Gou, W., Li, H., Yang, X., Fang, Y., Long, B., & Liu, S. (2019). Expression of the Proteins Ski and Akradia in the Retinal Tissue of Diabetic Rats. Nanoscience and Nanotechnology Letters, 11(12), 1693-1698.

[9] Huang, Y., Mo, F. M., Zou, J., Fang, P., Pan, Y., Zhu, X., Wang, D., & Xiao, P. (2019). A Comparative Study of the Calcium Carbonate Nanoparticles and the Chelators on Blood Lead Level Reduction and the Side Effects. *Nanoscience and Nanotechnology Letters, 11(8)*, 1145-1152.

[10] Irshad, A., Zhu, L., Huma, B., Asad, A., & Liu, Q. (2019). Electrical Sensing and Discrimination of Different States of Myoglobin Through Solid-State Nanopore. *Nanoscience and Nanotechnology Letters, 11(9)*, 1271-1280.

[11] Jiang, D., Chen, F. X., Zhou, H., Lu, Y. Y., Tan, H., Yu, S. J., Yuan, J., Liu, H., Meng, W., & Jin, Z. B. (2020). Bioenergetic crosstalk between mesenchymal stem cells and various ocular cells through the intercellular trafficking of mitochondria. Theranostics, 10(16), 7260.

[12] Kamran, M., Khan, M. A., Shafique, M., Ahmed, W., & Ahmad, S. (2019). Development and Characterization of Binary Solid Lipid Nano Suspension of Atorvastatin: In-Vitro Drug Release and In-Vivo Pharmacokinetic Studies. Nanoscience and Nanotechnology Letters, 11(11), 1522-1530.

[13] Lee, S. H., Cho, J. H., & Kim, H. E. (2017). Effect of Coronary Artery Calcification Score by Lifestyle and Correlation With Coronary Artery Stenosis by Multidetector Computed Tomography. *Journal of Computer Assisted Tomography, 41(02)*:236-236.

[14] Li, J., Zhao, P., Zhao, Y., Tian, L., Tian, Z., & Wang, C. (2019). Characteristics of Anti-Fungal Activity to Alternaria alternate of Different Proportion of Extraction from Sunflower Discs and Stalks. Nanoscience and Nanotechnology Letters, 11(11), 1561-1565.

[15] Li, J., Li, M., & Wang J. (2017). The relationship between left ventricular strain and transmural degree of acute myocardial infarction measured by magnetic resonance imaging feature tracking technique. *Chinese Journal of Interventional Cardiology*, 25(12):664-670.

[16] Li, Jianan, Zhang, L., & He, Y. (2017). Progress of cardiac magnetic resonance imaging in the diagnosis of myocardial activity in patients with chronic total coronary artery occlusion. *Chinese Journal of Interventional Cardiology*, 25(09):525-527.

[17] Li, X., Zhang, R., Zhang, X., Zhu, P., & Yao, T. (2020). Silver-Catalyzed Decarboxylative Allylation of Difluoroarylacetic Acids with Allyl Sulfones in Water. Chemistry–An Asian Journal, 15(7), 1175-1179.

[18] Liu, G., Ren, G., Zhao, L., Cheng, L., Wang, C., & Sun, B. (2017). Antibacterial activity and mechanism of bifidocin A against Listeria monocytogenes. Food Control, 73, 854-861.

[19] Liu, H., Liu, X., Zhao, F., Liu, Y., Liu, L., Wang, L., Geng, C., & Huang, P. (2020). Preparation of a hydrophilic and antibacterial dual function ultrafiltration membrane with quaternized graphene oxide as a modifier. Journal of Colloid and Interface Science, 562, 182-192.

[20] Liu, L., Li, J., Yue, F., Yan, X., Wang, F., Bloszies, S., & Wang, Y. (2018). Effects of arbuscular mycorrhizal inoculation and biochar amendment on maize growth, cadmium uptake and soil cadmium speciation in Cd-contaminated soil. Chemosphere, 194, 495-503.

[21] Liu, Y., Jiang, J., Ye, Y., Li, Z., Tan, M., Zou, J., & Hu, K. (2019). Stromal Vascular Fraction and Platelet-Rich Plasma Upregulate Vascular Endothelial Growth Factor Expression to Promote Hair Growth via the Wnt/β-Catenin Signaling Pathway. Nanoscience and Nanotechnology Letters, 11(12), 1685-1692.

[22] Loya-Rivera, M., Garcia-Ruiz, S. C., Flores-Holguín, N., Orrantia-Borunda, E., Chavez-Flores, D., & Luna-Velasco, A. (2019). Tamoxifen-Loaded Nanodiamonds as a Potential Nanosystem for Drug Delivery to Breast Cancer Cells. *Nanoscience and Nanotechnology Letters*, 11(8), 1131-1138.

[23] Lu, G., Hao C., & Wang Z. (2017). Evaluation of the efficacy of autologous bone marrow stem cell transplantation for myocardial infarction at different time points after coronary artery bypass grafting. *Chinese Journal of Nuclear Medicine and Molecular Imaging*, 37(06):321-321.

[24] Luo, Y., Zeng W., & Chen B. (2018). Diagnostic value of MSCT coronary CT angiography combined with CMR in myocardial ischemia of coronary heart disease. *Medical Review*, 24(14):178-182.

[25] Ma, M., Zhu Y., & He Y. (2017). Progress in the application of cardiac magnetic resonance perfusion imaging in coronary artery disease. *Journal of Clinical Cardiovascular Diseases*, 33(03):12-15.

[26] Mou, X., Sheng, D., Bao, Z., Su, F., Fan, X., Zhu, Y., Ye, K., & Liu, H. (2019). Correlation Between Genotypes and Allele Frequency of Lymphotoxin-Alpha and Gastric Cancer via Magnetic Separation Dual-Color Fluorescent Genotyping. *Nanoscience and Nanotechnology Letters*, 11(10), 1457-1463.

[27] Multinational, S., Liu, T., & Dai, X. (2018). Evaluation of the Diagnostic Value of Cardiac Magnetic Resonance Tissue Tracking in Patients with Coronary Heart Disease and Myocardial Infarction. *Magnetic resonance Imaging*, 71(05):36-43.

[28] Pan, D., Xia, X. X., Zhou, H., Jin, S. Q., Lu, Y. Y., Liu, H., Gao, M. L., & Jin, Z. B. (2020). COCO enhances the efficiency of photoreceptor precursor differentiation in early human embryonic stem cell-derived retinal organoids. Stem cell research & therapy, 11(1), 1-12.

[29] Ran, H., Wang Z., & He, Y. (2017). Diagnostic value of cardiac magnetic resonance imaging in viral myocarditis with main manifestations of the acute coronary syndrome. *Magnetic resonance Imaging*, 33(08):578-582.

[30] Shao, H., Sun, Y., & Ma, W. (2018). Meta-analysis of the accuracy of different types and magnetic field intensity cardiac magnetic resonance imaging in the diagnosis of coronary artery disease. *Chinese Journal of Evidence-based Medicine*,18(04): 315-325.

[31] Si, S., Li, L., Wang, Z., Wu, Y., Shan, G., Xu, B., Qin, Y., Duan, R., & Song, S. (2019). Cerium Oxide Nanoparticles Reduce X-ray Irradiation-Induced Damage to the Immune Cells by Upregulation of Superoxide Dismutase and Glutathione Peroxidase. Nanoscience and Nanotechnology Letters, 11(10), 1464-1469.

[32] Su, F., Jia, Q., Li, Z., Wang, M., He, L., Peng, D., ong, Y., Zhang, Z., & Fang, S. (2019). Aptamer-templated silver nanoclusters embedded in zirconium metal–organic framework for targeted antitumor drug delivery. Microporous and Mesoporous Materials, 275, 152-162.

[33] Su, Q., Liu, Y., Lv, X. W., Dai, R. X., Yang, X. H., & Kong, B. H. (2020). LncRNA TUG1 mediates ischemic myocardial injury by targeting miR-132-3p/HDAC3 axis. *American Journal of Physiology-Heart and Circulatory Physiology, 318(2),* H332-H344.

[34] Wan, Q., Chen, X., Geng, J., & Zhao, X. (2019). The Contrast Research of Human Papillomavirus Infection Genotypes in Tissues of Cervical Squamous Cell Carcinoma and Cervical Adenocarcinoma. Nanoscience and Nanotechnology Letters, 11(11), 1595-1602.

[35] Wang, M., Hu, M., Li, Z., He, L., Song, Y., Jia, Q., Zhang, Z., & Du, M. (2019). Construction of Tb-MOF-on-Fe-MOF conjugate as a novel platform for ultrasensitive detection of carbohydrate antigen 125 and living cancer cells. *Biosensors and Bioelectronics*, 142, 111536.

[36] Wang, W., Zhang, G., & Wang, X. (2018).

Progress in the application of coronary flow reserve in coronary microangiopathy. *Chinese Medical Imaging Technology*,34(11):125-128.

[37] Xiao, J., Zhao, Y., & Zhang, C. (2019). Application of Serum Thymidine Kinase-1 in Cancer Risk Detection in Healthy Population. Nanoscience and Nanotechnology Letters, 11(12), 1734-1738.

[38] Xu, L., Lu, Z., Tan, G. H., Huang, F. Y., Cao, R., He, N., Xu, T., & Zhang, L. (2019). Coomassie Bright Blue-Conjugated Human Serum Albumin Nanoparticles as a Tumor-Selective Weapon for Leukemia Therapy. *Nanoscience and Nanotechnology Letters*, *11(12),* 1651-1660.

[39] Xu, X., Xiao, L., Zhang, J., Luo, D., Wang, L., Peng, Z., Liao, D., Xing, C., Pu, W., & Li, K. (2019). A Modified Mutation-Sensitive On/Off Switch and Its Application in B-Raf Proto-Oncogene Hotspot Mutation Assay. Nanoscience and Nanotechnology Letters, 11(11), 1582-1588.

[40] Xu, Z., Wu, W., & Shang, C. (2019). Hypermethylation of BMP1 Promoter Regulates Migration of Colon Cancer Cells by Regulating the TGF-Beta 1/Smad2 Signaling Pathway. Nanoscience and Nanotechnology Letters, 11(12), 1711-1717.

[41] Yan, Y., Zhu, W., Cai, X., Fang, G., Cao, X., Jiang, W., Li, J., Xiao, F., Wu, Y., & He, N. (2019). Research on Diagnosis of Breast Cancer Based on Ultrasonic Radio Frequency Signals. Nanoscience and Nanotechnology Letters, 11(8), 1116-1124.

[42] Zhang, L., Song, X., & Dong, L. (2018). Additive value of 3T cardiovascular magnetic resonance coronary angiography for detecting coronary artery disease. Journal of Cardiovascular Magnetic Resonance, 20(01):29-29.

[43] Zhang, L., Zhang, H., Huang, Y., Zhang, J., Chen, X., Chen, Y., Miao, G., & Cui, D. (2019). Detection of Kappa Light Chain Protein in Human Urine by Surface Plasmon Resonance. *Nanoscience and Nanotechnology Letters*, *11(12),* 1666-1670.

[44] Zhang, X. L., Zhu, Q.Q., & Yang, J. J. (2017). Percutaneous intervention versus coronary artery bypass graft surgery in left main coronary artery stenosis: a systematic review and meta-analysis. *Bmc Medicine*, 15(01):84.

[45] Zhang, X., Xia, C., & Li, S. (2019). Efficacy of Cortex Mori–Liuwei Dihuang Nanoparticle Pills on Renal Interstitial Fibrosis via TGF-β/Smad Signaling. *Nanoscience and Nanotechnology Letters*, *11(12),* 1661-1665.

[46] Zhao, Y., Zhao, P., Luo, J., Tian, L., Tian, Z., & Li, J. (2019). Effects of Different Hormone Concentrations on Callus Induction of Astragalus mongholicus Bunge. *Nanoscience and Nanotechnology Letters*, *11(12),* 1729-1733.

[47] Zhong, P. F., Lin, H. M., Wang, L. W., Mo, Z. Y., Meng, X. J., Tang, H. T., & Pan, Y. M. (2020). Electrochemically enabled synthesis of sulfide imidazopyridines via a radical cyclization cascade. *Green Chemistry*, *22(19),* 6334-6339.

[48] Zhou, D., Luo, J., Sun, T., Ni, H., & Yu, X. (2019). Development of a Panel of Six Duplex Real-Time Reverse Transcription Polymerase Chain Reaction Assays for Detecting 12 Mosquito-Borne Viruses. Nanoscience and Nanotechnology Letters, 11(1), 136-142.

[49] Zhou, S., Qiao, Y., & Wang, S. (2017). Value of contrast-enhanced delayed cardiac magnetic resonance imaging in prognosis evaluation of patients undergoing coronary artery bypass surgery. *Chinese Journal of Practical Diagnosis and Treatment*,31(05):470-472.

[50] Zhou, S., Zeng, H., & Wang, W. (2019). An Overview of Stability Analysis of Neural Networks with Time-Delays. *Nanoscience and Nanotechnology Letters*, *11(9),* 1200-1212.

[51] Zhu, M., Lai, X., Wen, Y., & Zhang, H. (2019). The Efficacy of Adipose-Derived Stem Cells (ADSCs) on Chronic Kidney Disease in Dogs. *Nanoscience and Nanotechnology Letters*, *11(12),* 1724-1728.

[52] Zuo, C., Chen, Q., Gu, G., Feng, S., Feng, F., Li, R., & Shen, G. (2013). High-speed three-dimensional shape measurement for dynamic scenes using bi-frequency tripolar pulse-width-modulation fringe projection. *Optics and Lasers in Engineering*, *51(8),* 953-960.

[53] Zuo, C., Chen, Q., Tian, L., Waller, L., & Asundi, A. (2015). Transport of intensity phase retrieval and computational imaging for partially coherent fields: The phase space perspective. *Optics and Lasers in Engineering*, *71*, 20-32.

[54] Zuo, C., Sun, J., Li, J., Zhang, J., Asundi, A., & Chen, Q. (2017). High-resolution transport-of-intensity quantitative phase microscopy with annular illumination. *Scientific reports*, *7(1),* 1-22.